

High degrees of melt extraction recorded by spinel harzburgite of the Newfoundland margin: The role of inheritance and consequences for the evolution of the southern North Atlantic

Othmar Müntener^{a,*}, Gianreto Manatschal^b

^a *Institute of Geological Sciences, University of Bern, Baltzerstr. 1-3, CH-3012 Bern, Switzerland*

^b *CGS-EOST, Université Louis Pasteur, 1 rue Blessig, F-67084 Strassbourg, France*

Received 11 May 2006; received in revised form 19 September 2006; accepted 3 October 2006

Available online 13 November 2006

Editor: R.D. van der Hilst

Abstract

Serpentinized spinel peridotites of the Newfoundland margin drilled during ODP Leg 210 at Site 1277 have preserved, relic mineral compositions similar to the most depleted abyssal peridotites worldwide and different from those of the conjugate Iberian margin. The samples are derived from mass flows containing clasts of peridotite and gabbro and from in-situ basement, and are mostly mylonitic cpx-poor spinel harzburgites with Cr-rich spinels ($Cr\#_{0.35-0.66}$). Melting of the Newfoundland mantle occurred in the spinel peridotite field and probably exceeded the cpx-out phase boundary for some samples. Using proposed spinel peridotite melting models and experimentally derived phase diagrams, the Newfoundland harzburgites can be modeled as a residue after extraction of 14 to 20–25% melting. Basalts that are interleaved with mass flow deposits on top of the peridotite basement resemble normal to transitional mid-ocean ridge basalt. This, together with the unusually high Cr# of some spinel harzburgites suggest that the formation of basalts and partial melting of the underlying peridotite are not cogenetic. Among mantle samples some of the Newfoundland harzburgites approach mineral compositions of the Bay of island ophiolite and ophiolites from Japan that represent peridotites formed in an arc-setting. Thus, the peridotites drilled at Site 1277 may represent inherited (Caledonian or older) subarc mantle that was exhumed close to the ocean floor during the rifting evolution of the Atlantic.

Compared to the spinel harzburgites from Newfoundland, the peridotites from the conjugate Iberian margin are, on average, less depleted and provide evidence for local equilibration in the plagioclase stability field. This can either be explained by an inherited, primary, Ca-richer composition of the Iberia peridotite, or, alternatively, by local melt impregnation and stagnation during continental rifting, and thus refertilizing previously depleted (arc-related) peridotite.

© 2006 Elsevier B.V. All rights reserved.

Keywords: Mantle melting; Newfoundland margin; ODP Leg 210; Spinel harzburgite

1. Introduction

Non-volcanic (or magma-poor) passive margins have been the subject of ongoing debates for the last 20 yr, since rift-related decompression of the mantle is generally considered to produce substantial amounts of

* Corresponding author. University of Lausanne, Institute of Mineralogy and Geochemistry, Anthropole, CH-1015 Lausanne, Switzerland. Tel.: +41 216924347; fax: +41 216924306.

E-mail address: othmar.muntener@unil.ch (O. Müntener).

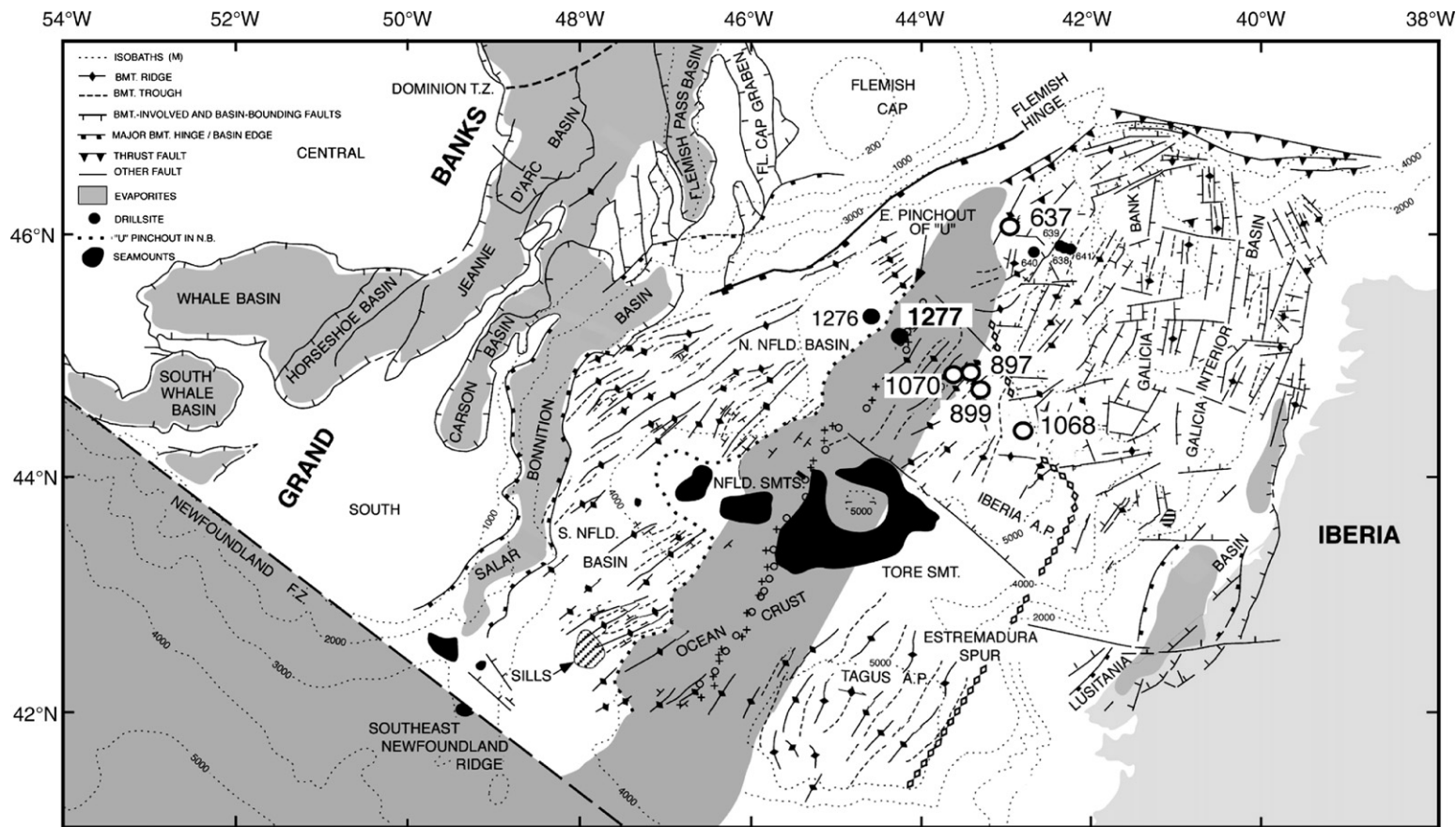


Fig. 1. Reconstruction of the Iberia–Newfoundland rift to anomaly M0 (~121 Ma), based on the reconstruction of [54]. Onset of oceanic crust formation was interpreted to initiate around magnetic anomaly M3 (grey shaded area). Solid circles indicate locations of drill Sites (1276, 1277) during ODP Leg 210. Open circles indicate locations of peridotite highs, which were drilled during previous ODP legs 103, 149 and 173, respectively. Modified from [19].

melts. The observation, that peridotites might be exhumed on the ocean floor without being covered by volcanic and/or plutonic products has long been known for some passive margins [1,2], but the recent discovery of basalt-‘free’ segments of (ultra-) slow mid-ocean ridges [3–7] demonstrates that both rifting and spreading are not necessarily expressed by volcanic activity at

the surface. The highly variable volumes of volcanic rocks produced during rifting and breakup of continents has led to the distinction of ‘volcanic’ and ‘non-volcanic’ passive margins, meaning that in some margins there is syn-rift decompression melting, while in others there isn’t. This concept, however, becomes invalid if substantial amounts of magma are stored at depth by

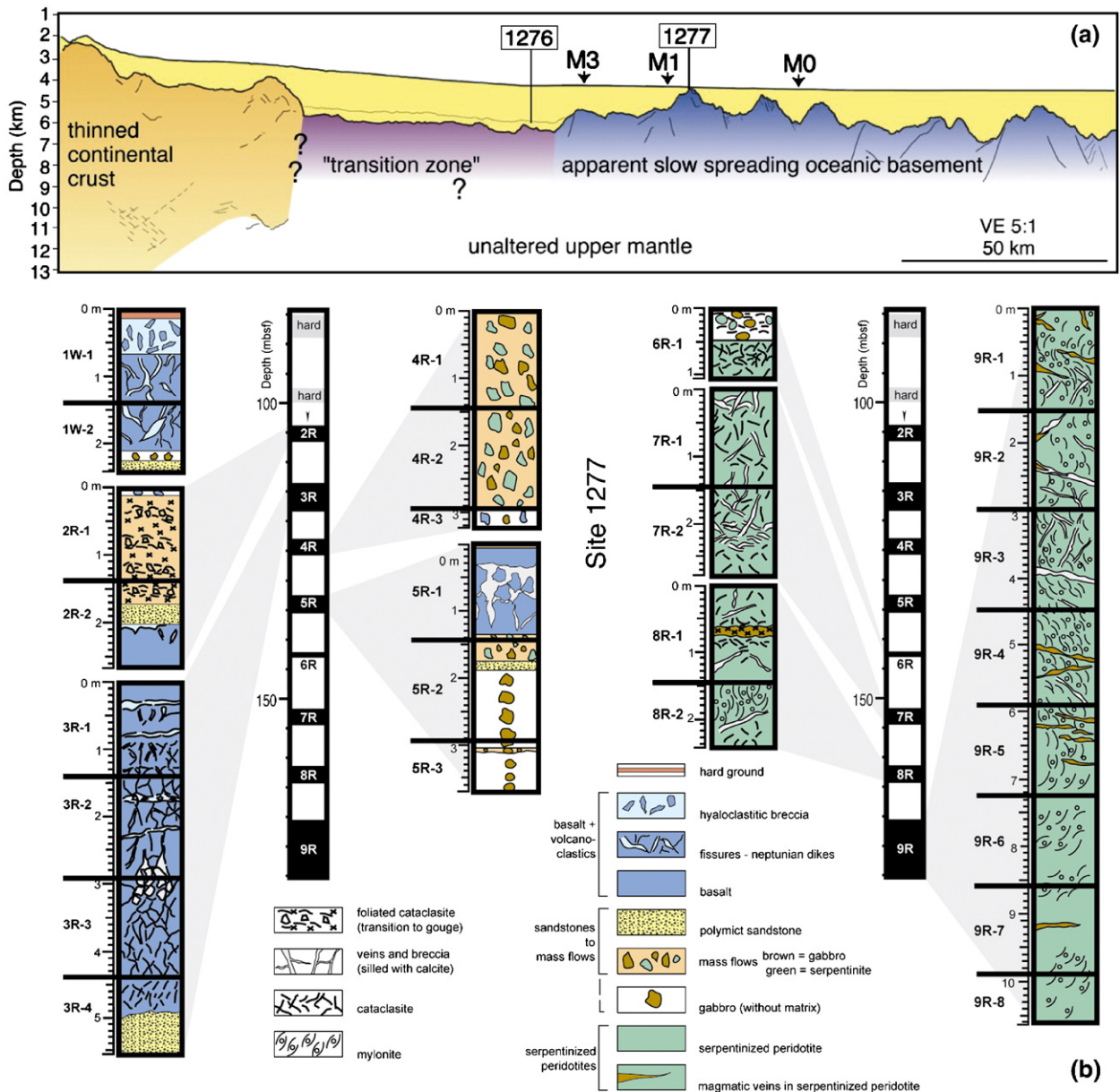


Fig. 2. (a) Tentative geologic interpretation of the SCREECH 2 seismic reflection profiles [20,21]. The rough topography oceanwards of M3 marks apparent slow spreading oceanic basement. ODP Leg 210, Site 1277 cored about 80 to 100 m of apparent in-situ basement, just oceanwards of anomaly M1. (b) Detailed stratigraphy and recovery of Site 1277. The cores from the upper part show a complex assemblage of basalt flows interleaved with sandstones and mass flows containing clasts of mafic rocks and serpentized peridotite and variably deformed gabbroic rocks. The lower 40 m is made of serpentized peridotite and minor gabbroic to monzonitic veins.

Table 1
Locations and petrological characteristics of samples from ODP Leg 210, Site 1277

Core section (3)	Sample nr	Depth mbsf	Lithology (1)	Texture (2)	Primary min.
1W-2 95–98	z03	85–103 (3)	sb	pc	spl
1W-P6 101–104	1W-P6	85–103	sb	pc	spl
4R-1 11–14	4R-1	123.12	sb	pc, gb	ol, spl, cpx, opx
4R-1 34–38	z10	123.34	sb	pc	spl
7R-2 127–129	z29	154.5	spm+gv	pc	spl, cpx, opx
9R-1 117–120	z39	171.87	spm	pc	spl, cpx, opx
9R-4 33–36	z45	175.34	spm	pc	spl
9R-4 138–141	z47	176.39	spm	pc	spl, opx
9R-6 68–71	z51	178.4	spm+gv	pc	spl

(1) sb: sedimentary breccia with peridotite components; spm: serpentinized peridotite mylonite; gv: gabbroic veins.

(2) Denotes mineral textures: pc: porphyroclastic; gb: granoblastic.

(3) Sample depth of core 1W can only be estimated [19].

melt stagnation in the thermal lithosphere, which may be a common process in actual and ancient slow spreading systems (e.g. [8–10]).

On the other hand, some areas of the upper mantle are initially too depleted to produce substantial amounts of melt during decompression. This is because the solidus of peridotite increases by more than 100 °C between fertile upper mantle and the depleted upper mantle [11–13]. Thus, for a given mantle potential temperature (e.g. 1300 °C [14]), adiabatic decompression of fertile mantle might produce substantial volumes of syn-rift liquids, while decompression of depleted mantle remains relatively unproductive. In addition, considering a ‘cold’ mantle potential temperature of 1200 °C (e.g. [15]) further reduces the productivity of syn-rift decompression melting. Thus, magma-poor passive margins play a key role for investigating this process as they represent an interface between advanced rifting and early (ultra-) slow sea-floor spreading. Adiabatic decompression of the mantle might still be in its infancy and thus compositional and/or thermal effects of the underlying mantle are potentially reflected in the presence or absence of syn-rift melts.

In this paper, we concentrate on constraints from the conjugate Iberia–Newfoundland margin, to the genesis of peridotites in magma-poor passive margins. Dredging

and drilling of the Iberia margin has led to the proposal that the peridotites have a subcontinental origin, comparable to on-land peridotite massifs (e.g. Ronda, Lherz, [16–18]) and that the peridotites record a subsolidus exhumation history. Recent seismic interpretations of the conjugate Newfoundland margin have proposed the existence of exhumed, serpentinized mantle followed by very thin oceanic crust from magnetic anomaly M3 onward [20,21]. To explore these interpretations further we investigated serpentinized peridotites from the Newfoundland margin that were drilled during ODP Site 1277, providing the first dataset on peridotites from a conjugate magma-poor margin.

One aim of this study is to determine the degree of melting of peridotite for the conjugate Iberia–Newfoundland magma poor system. More generally, we evaluate the spatial variability of peridotite composition in a system, which is relevant for both advanced stages of rifting and earliest (ultra-) slow sea-floor spreading.

2. Site characteristics

ODP Leg 210, Site 1277 in the Newfoundland margin has penetrated about 80–100 m into a shallow basement high just on the oceanic side of magnetic anomaly M1 (~121 Ma, Figs. 1 and 2). Overall core

Fig. 3. Photomicrographs from serpentinized peridotites from ODP Leg 210, Site 1277. All images are taken with crossed polarizers. (a) Serpentinized peridotite mylonite (7R-2, 17–20), cut by undeformed talc-rich veins (1), serpentine veins (2) and calcite veins (3). Note the extremely stretched, altered orthopyroxene (opx) in the centre of the image. (b) spinel and opx porphyroclasts, set in a (serpentinized) mylonitic matrix (7R-2, 17–20). (c) Opx porphyroclast with clinopyroxene (cpx) exsolution lamellae, partially replaced by calcite. Note that ghosts of cpx exsolution lamellae are preserved in calcite (9R-3 119–123). (d) opx porphyroclast, set in a matrix of dynamically recrystallized opx, cpx, spinel and olivine (4R-1, 11–14). (e) opx porphyroclast with coarse exsolution lamellae of cpx, surrounded by partially serpentinized spinel peridotite (ol, spl, opx, cpx) assemblages (4R-1 11–14). (f) Oxide gabbro with coarse cpx, plagioclase and ilmenite phenocrysts, and a finegrained cpx + Ti-hornblende matrix. Note the deformed twin lamellae of large plagioclase, and the undeformed, small neoblasts, indicating dynamic recrystallization (z01). (g) Idiomorphic zircon in small gabbro vein, together with apatite (ap), plagioclase (plg) and twinned Mg-hornblende (hbl) (9R-6, 68–71). (h) mafic igneous vein, with biotite (bt) and plagioclase (plg) (z36).

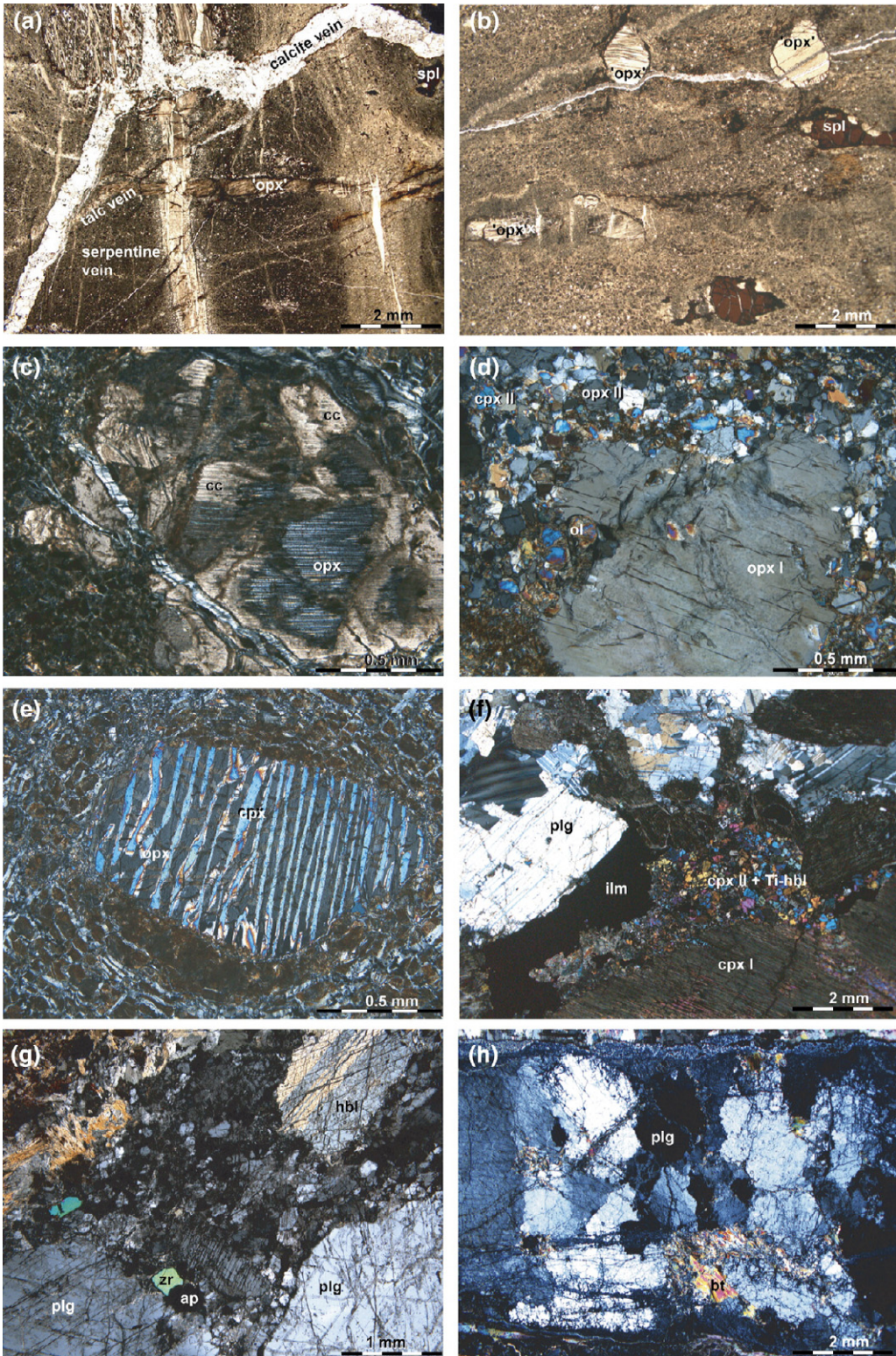


Table 2

Major element concentrations (wt.%) in spinel from peridotites of ODP Leg 210, Site 1277

Sample	z51_1		z51_5		z51_6		z51_7		z10_1		z10_2		z10_3		z10_4	
Core section	9R-6 68–71						4R-1 34–38									
<i>n</i>	5	2σ	5	2σ	5	2σ	6	2σ	4	2σ	5	2σ	9	2σ	6	2σ
TiO ₂	0.02	0.01	0.06	0.03	0.04	0.02	0.03	0.02	0.12	0.01	0.04	0.02	0.04	0.01	0.03	0.02
Al ₂ O ₃	36.4	0.7	32.5	0.9	31.0	0.3	27.9	2.2	28.4	0.6	33.0	0.6	26.8	0.5	31.2	0.7
Cr ₂ O ₃	32.3	1.0	37.6	0.9	37.0	0.3	36.5	1.5	41.9	0.6	36.5	0.8	40.7	0.5	37.5	0.2
Fe ₂ O ₃	1.41	0.24	0.73	0.53	1.85	0.18	3.40	0.18	0.33	0.32	0.92	0.39	1.93	0.53	1.66	0.78
FeO	13.5	0.3	13.2	0.5	15.6	0.4	20.6	1.2	13.7	0.3	13.4	0.4	20.2	0.7	13.7	1.0
MnO	0.13	0.01	0.14	0.00	0.15	0.01	0.17	0.02	0.14	0.01	0.16	0.01	0.17	0.01	0.15	0.01
NiO	0.13	0.03	0.15	0.04	0.11	0.03	0.13	0.02	0.15	0.06	0.11	0.04	0.08	0.02	0.18	0.02
MgO	15.3	0.1	14.9	0.7	13.4	0.2	9.5	1.2	14.4	0.1	15.0	0.3	10.1	0.5	14.5	0.6
Σ	99.6		99.7		99.6		99.6		99.6		99.7		100.1		99.5	
Cr#	0.373		0.437		0.444		0.468		0.498		0.426		0.504		0.447	
Mg#	0.646		0.654		0.576		0.415		0.643		0.649		0.447		0.627	
Sample	z10_6		4R-1_1		4R-1_5		4R-1_3		4R-1_6		1WP-6_1		1WP-6_4		1WP-6_3	
Core section	4R-1 11–14						1W-P6 101–104									
<i>n</i>	10	2σ	6	2σ	6	2σ	2	2σ	5	2σ	10	2σ	9	2σ	10	2σ
TiO ₂	0.08	0.02	0.11	0.02	0.13	0.02	0.12	0.01	0.08	0.03	0.03	0.02	0.06	0.01	0.02	0.01
Al ₂ O ₃	32.3	0.5	19.0	0.1	18.4	0.1	26.3	0.6	23.6	0.4	30.2	0.2	30.7	0.2	30.5	0.8
Cr ₂ O ₃	38.7	0.2	50.4	0.3	50.8	0.4	42.1	0.1	45.1	0.4	38.9	0.3	39.4	0.3	37.0	0.9
Fe ₂ O ₃	1.01	0.34	1.75	0.20	2.05	0.14	2.18	0.08	1.81	0.27	2.29	0.29	0.69	0.24	2.79	0.58
FeO	12.3	0.2	16.0	0.2	15.8	0.3	18.5	0.2	17.3	0.2	12.2	0.3	12.8	0.3	14.9	1.8
MnO	0.16	0.00	0.18	0.01	0.18	0.01	0.16	0.01	0.16	0.01	0.14	0.01	0.14	0.01	0.13	0.01
NiO	0.14	0.07	0.07	0.03	0.05	0.02	0.05	0.02	0.06	0.05	0.15	0.04	0.12	0.04	0.13	0.03
MgO	16.0	0.1	11.9	0.1	12.0	0.1	11.4	0.1	11.6	0.1	15.6	0.2	15.2	0.2	13.8	1.4
Σ	100.7		99.4	0.2	100.1	0.6	100.8	0.6	99.7	0.4	99.5	0.4	99.1	0.3	99.3	0.8
Cr#	0.446		0.641		0.649		0.518		0.562		0.464		0.463		0.449	
Mg#	0.680		0.544		0.545		0.493		0.518		0.657		0.666		0.581	

Each measurement represents an average of a single grain. Mg# (molar Mg/Mg+Fetot); Cr# (molar Cr/Cr+Al).

Per: spinels from peridotite, brecc: spinels from breccias; *n*: number of analyses; 2σ: standard deviation of the mean.

Fe₂O₃ calculated by stoichiometry (3 cations, 8 charges).

recovery is ~60%. Two lithologic units might be recognized (Fig. 2b, see also [19]): (1) Cores from the upper part (~85–142 mbsf) show a complex assemblage of basalt flows (50%) interleaved with sandstones (10%) and mass flows containing clasts of mafic rocks and serpentinized peridotite (~20%) and variably deformed gabbroic rocks (~20%). The material from the sedimentary layers is interpreted to be derived exclusively from the underlying basement [19]. (2) The lower 40 m of the drilled material represents in-situ basement and consists of serpentinized peridotite plus minor gabbroic veins (less than 5%). Based on detailed refraction seismic investigations it was concluded that this part of the basement represents (a) serpentinized peridotite or (b) (ultra-) slow spreading oceanic crust [19–21].

The entire ultramafic section is extensively serpentinized (>90%). The pebbles from the mass flows between 100 to 140 m depth are strongly serpentinized, weakly deformed to mylonitic harzburgites. No dunites or py-

roxenites have been identified, although the high degree of serpentinization makes the classification somewhat difficult. The matrix of the mass flow deposits is poorly sorted and often composed of a serpentine–carbonate matrix, with relic, fresh, mantle spinel and gabbro cpx grains and, occasionally, with pseudomorphs of pyroxenes. Secondary chlorite, and fibrous tremolite are found along the contact to clinopyroxene.

3. Results

3.1. Petrography and microstructural observations

The samples investigated for this study were collected by deep sea drilling during ODP Leg 210 (Site 1277) along the Newfoundland margin [19]. Out of 25 samples, nine were analyzed in detail. They comprise four breccias containing serpentinized peridotite clasts and five samples from the solid serpentinized peridotite in the lower part of Site 1277. The downhole location of the different samples

z47_3		z47_4		z47_5		z47_6		z45_1		z45_1		z45_5		z03_1	
9R-4 138–141								9R-4 33–36						1W-2 95–98	
5	2 σ	5	2 σ	5	2 σ	6	2 σ	10	2 σ	5	2 σ	10	2 σ	5	2 σ
0.04	0.02	0.03	0.02	0.03	0.02	0.02	0.02	0.04	0.02	0.05	0.01	0.05	0.02	0.03	0.03
36.6	0.9	35.9	0.9	36.5	0.2	38.3	0.6	31.5	0.2	31.1	0.2	29.9	0.2	33.3	0.3
33.6	0.9	34.1	0.9	33.5	0.2	31.3	0.4	39.2	0.3	39.7	0.3	40.4	0.2	35.6	0.4
1.14	0.19	1.23	0.22	1.03	0.20	1.12	0.37	1.18	0.13	0.95	0.09	1.53	0.25	1.46	0.41
11.1	0.2	11.7	0.4	11.7	0.1	11.8	0.3	12.9	0.1	12.8	0.2	12.5	0.3	15.1	0.4
0.14	0.01	0.15	0.01	0.15	0.01	0.14	0.01	0.15	0.01	0.16	0.01	0.17	0.01	0.57	0.02
0.18	0.02	0.17	0.03	0.16	0.04	0.12	0.03	0.15	0.05	0.08	0.06	0.15	0.04	0.11	0.08
17.1	0.2	16.5	0.4	16.6	0.1	16.8	0.1	15.5	0.1	15.5	0.1	15.4	0.2	14.2	0.4
99.9		99.5		99.6		99.6		100.7		100.3		100.1		100.3	
0.381		0.389		0.382		0.354		0.455		0.461		0.476		0.418	
0.711		0.693		0.698		0.698		0.662		0.665		0.661		0.603	
z03_2		z39_1		z39_2		z39_3		z39_4		z29_1		z29_2		z29_3	
		9R-1 117–120								7R-2 127–129					
		5	2 σ	3	2 σ	3	2 σ	3	2 σ	3	2 σ	3	2 σ	3	2 σ
0.05	0.01	0.08	0.02	0.08	0.03	0.07	0.01	0.06	0.02	0.02	0.02	0.24	0.03	0.03	0.01
31.9	0.4	32.3	0.5	31.1	0.5	31.1	0.5	33.9	0.2	35.4	0.3	30.5	0.3	36.5	0.9
38.0	0.3	38.7	0.2	40.0	0.4	39.1	0.9	36.2	0.1	34.3	0.2	38.7	0.4	32.7	0.5
0.60	0.59	1.01	0.34	1.04	0.64	1.16	0.55	0.73	0.15	1.37	0.12	1.87	0.01	1.64	0.87
15.6	0.5	12.3	0.2	12.5	0.7	13.1	0.8	13.7	0.3	12.8	0.1	13.8	0.2	13.2	0.7
0.62	0.03	0.16	0.00	0.15	0.01	0.16	0.00	0.15	0.00	0.13	0.01	0.16	0.01	0.13	0.01
0.12	0.06	0.14	0.07	0.14	0.04	0.08	0.06	0.13	0.04	0.13	0.01	0.15	0.07	0.12	0.03
13.7	0.3	16.0	0.1	15.8	0.2	15.3	0.5	15.1	0.1	15.8	0.2	14.8	0.1	15.7	0.4
100.6		100.7		100.8		100.1		100.0		100.0		100.2		100.1	
0.445		0.446		0.464		0.457		0.417		0.395		0.460		0.376	
0.598		0.680		0.674		0.655		0.650		0.664		0.627		0.653	

is summarized in Table 1, together with the textures and the primary mineralogy. All samples are strongly (>90%) serpentinized, and locally pyroxenes show topotactic overgrowths by carbonate. At least three generations of late veins (talca, serpentine+magnetite, and carbonate veins, respectively) are crosscutting the peridotites (Fig. 3a).

Texturally, the spinel harzburgites are porphyroclastic to mylonitic with mainly coarse orthopyroxene and spinel porphyroclasts in the 0.5–1.5 mm range (Fig. 3b), embedded in a mylonitic matrix. The shape of orthopyroxene porphyroclasts depends on the orientation of the (001) exsolution lamellae, varying from rounded clasts to extremely stretched crystals, with aspect ratios exceeding 10:1 (Fig. 3a). Orthopyroxene porphyroclasts always show fine clinopyroxene exsolution lamellae, which are mostly replaced by calcite. A representative example of calcitized orthopyroxene is shown in Fig. 3c. Apart from these normal and representative textures, sedimentary breccias contain spinel clasts, and occasionally serpenti-

nized peridotite fragments (less than 2 cm in diameter). These fragments show the same porphyroclastic textures as in the in-situ basement. We conclude that the breccias are representative of the mantle drilled at Site 1277 (see Section 4).

The mylonitic matrix surrounding and partially replacing opx porphyroclasts is composed of dynamically recrystallized ortho- and clinopyroxene, spinel and olivine (Fig. 3d). Fresh olivine has only been found in one sample (Table 2).

Fresh clinopyroxene has only been observed as small grains (<100 μm) in the recrystallized mylonitic matrix, and as exsolution lamellae within orthopyroxene (Fig. 3c, e). Exsolution lamellae usually have relatively constant thickness (<10 μm) and disappear towards the grain boundaries, except in one sample coarse clinopyroxene exsolutions (up to 0.1 mm) are preserved (Fig. 3e). This unusual texture resembles exsolved pigeonitic pyroxene, and both orthopyroxene host and clinopyroxene lamellae are among the most depleted ones drilled so

Table 3

Major element concentrations in olivine and pyroxene from peridotites of ODP Leg 210, Site 1277

Sample	ol		ol		cpx		cpx		cpx		cpx		cpx		cpx	
	4R-1_1		4R-1_2		4R-1_4		4R-1_3		4R-1_2		z39_1		z39_2		z29_3	
Location	gb		gb		gb		exsol		gb		gb		gb		gb	
<i>n</i>	7	2σ	4	2σ	4	2σ	4	2σ	4	2σ	5	2σ	4	2σ	5	2σ
SiO ₂	40.9	0.1	40.7	0.1	53.9	0.2	54.0	0.1	54.4	0.1	53.4	0.6	53.2	0.1	52.4	0.02
TiO ₂	0.01	0.01	0.01	0.03	0.07	0.02	0.04	0.02	0.05	0.02	0.08	0.02	0.08	0.05	0.09	0.01
Al ₂ O ₃	0.00	0.00	0.01	0.01	1.32	0.11	1.34	0.02	1.10	0.06	2.74	0.19	2.49	0.35	3.40	0.05
Cr ₂ O ₃	0.00	0.00	0.03	0.03	0.61	0.08	0.83	0.08	0.58	0.05	1.11	0.08	1.03	0.13	1.12	0.03
FeO	8.60	0.19	8.66	0.17	2.04	0.11	1.84	0.07	1.95	0.11	1.91	0.14	1.71	0.04	1.82	0.09
MnO	0.18	0.01	0.19	0.05	0.13	0.03	0.11	0.05	0.08	0.04	0.13	0.02	0.11	0.06	0.13	0.02
NiO	0.31	0.04	0.32	0.02	0.00	0.01	0.01	0.02	0.04	0.02	0.04	0.04	0.02	0.03	0.05	0.04
MgO	50.3	0.2	50.3	0.2	17.8	0.1	17.7	0.1	17.9	0.1	17.2	0.2	17.1	0.2	16.5	0.1
CaO	0.01	0.01	0.06	0.03	23.7	0.2	23.7	0.0	23.7	0.3	23.0	0.4	23.0	0.1	23.5	0.2
Na ₂ O	n.a.		n.a.		0.34	0.01	0.37	0.01	0.27	0.01	0.46	0.04	0.44	0.03	0.27	0.02
Σ	100.3		100.3		99.9		99.9		100.1		100.0		99.2		99.2	
Cr#					0.238		0.294		0.263		0.213		0.216		0.181	
Mg#	0.912		0.912		0.939		0.945		0.942		0.941		0.947		0.942	

Sample	oxp		opx		opx		opx		opx		opx		opx		opx	
	4R-1_2		4R-1_5		4R-1_4		Z39_2		Z47_2		Z47_1		z29_2		z29_1	
Type	gb		pc		rim		pc		pc		pc		pc		pc	
<i>n</i>	7	2σ	5	2σ	6	2σ	3	2σ	4	2σ	3	2σ	1		1	
SiO ₂	57.7	0.4	56.7	0.1	57.3	0.4	56.1	0.2	56.4	0.7	56.5	0.2	56.6		57.2	
TiO ₂	0.03	0.03	0.05	0.03	0.05	0.03	0.04	0.02	0.02	0.02	0.04	0.01	0.00		0.05	
Al ₂ O ₃	0.71	0.07	1.14	0.04	1.11	0.08	2.51	0.08	2.84	0.07	3.06	0.10	2.78		2.76	
Cr ₂ O ₃	0.24	0.07	0.53	0.03	0.40	0.07	0.78	0.05	0.82	0.08	0.86	0.06	0.76		0.83	
FeO	5.78	0.12	5.61	0.00	5.68	0.17	4.97	0.16	5.38	0.18	5.26	0.04	5.44		5.52	
MnO	0.18	0.03	0.17	0.07	0.19	0.03	0.14	0.03	0.17	0.04	0.18	0.02	0.22		0.16	
NiO	0.06	0.02	0.06	0.03	0.06	0.02	0.09	0.04	0.10	0.03	0.10	0.02	0.12		0.02	
MgO	35.1	0.3	34.3	0.1	35.0	0.3	33.6	0.2	33.9	0.5	34.2	0.2	32.8		33.3	
CaO	0.44	0.05	1.19	0.13	0.57	0.04	1.59	0.03	0.82	0.05	0.61	0.07	1.26		0.51	
Na ₂ O	0.01	0.01	0.04	0.12	0.01	0.01	0.07	0.02	0.02	0.01	0.00	0.01	0.06		0.01	
Σ	100.2		99.9		100.4		100.8		100.5		100.7		100.1		100.3	
Cr#	0.183		0.238		0.196		0.173		0.162		0.159		0.155		0.168	
Mg#	0.915		0.915		0.916		0.923		0.918		0.921		0.915		0.915	

Concentrations reported in wt.%; n.a. not analyzed; pc: porphyroclast core; gb: granoblast in mylonitic matrix; exsol: exsolved from opx; *n*: number of analyses; 2σ: standard deviation of the mean.

far (see below). The exclusive occurrence of clinopyroxene in the matrix suggests that some of the spinel harzburgites were virtually cpx-free, and that most clinopyroxene probably exsolved from orthopyroxene.

The breccias in the upper part of Site 1277 contain numerous clasts of gabbroic rocks ranging from gabbros, gabbronorites to oxide gabbros and anorthosites (Fig. 3f). They are composed of variable proportions of clinopyroxene (Mg# < 80), plagioclase (an50–65), ilmenite, Ti-pargasite and rare biotite and sulfides. Mm-scale monzonitic clasts containing Mg-hornblende, plagioclase (an8–14), potassium feldspar (or56–67, ab31–40, an2–4), and rare, idiomorphic Ba-feldspar (hyalophane), included in potassium feldspar (ce26–34, kfsp66–74, ab1–2), zircon and rutile are occasionally

associated with ultramafic pebbles embedded in a carbonate–serpentinite matrix. Actinolite and pure potassium feldspar are probably alteration products of the monzonitic veins. Thin potassium feldspar veins occasionally cut gabbroic pebbles, supporting the interpretation that pure Kfspar is related to alteration.

The peridotite basement is cut by gabbroic veins ranging in size from 2–3 mm to 3 cm maximum thickness. In general, they show a 1 to 2 mm hydrothermal reaction rim, marked by acicular tremolitic amphibole and chlorite. Two types of igneous veins can be distinguished: (a) zircon- and Cl-apatite-bearing plagioclase (An31–35)–hornblende veins (Fig. 3g) and (b) biotite–plagioclase–rutile–zircon (± monazite and xenotime) bearing veins (Fig. 3h). The hornblende-bearing veins are 113 ± 2 Ma

(U–Pb on zircon, [22]), postdating continental break-up, by approximately 10 Ma, while biotite-bearing rocks gave 126.5 Ma (Ar–Ar on biotite, [22]), an age slightly older than the presumed age of anomaly M3.

3.2. Major element mineral chemistry

Mineral compositions were determined using a Cameca SX-50 electron microprobe located at the Institute of Geological Sciences at the University of Bern (Switzerland), equipped with four wavelength-dispersive spectrometers. Operating conditions comprised an acceleration voltage of 15 kV and a 20 nA beam current. The spot size was about 2 μm for all minerals. Element peak and background counting time on either side of the peak was 20 s, except for Ni (40 s) and Na (10 s). Natural and synthetic oxides were used as standards. Where possible, four to eight points were measured in the core of the minerals, and averages and standard deviations are reported in Tables 2 and 3, respectively. Each grain was checked for core–rim zoning, and in most cases the minerals were homogeneous. Larger spinel grains in some samples show appreciable zoning, with a small increase of Mg# and a decrease in Cr#.

Fresh olivine crystals ($\text{Fo}_{91.2}$) have only been found in one peridotite clast (Table 3). Nickel in olivine ranges from 0.31 to 0.32 wt.% NiO.

Orthopyroxene is present in most samples, but is only rarely preserved. Mg# for all samples display little variation (0.914 to 0.922) and seems independent of the Cr# (0.155–0.238). Cr_2O_3 varies between 0.53 and 0.86 wt.%, while recrystallized opx in the mylonitic matrix shows substantially lower values (~ 0.25 wt.%). Intracrystalline zoning has only been observed in samples with preserved porphyroclasts and neoblasts. There, rim compositions of large porphyroclasts approach recrystallized grains, indicating retrograde equilibration.

Clinopyroxene has been found in 3 samples. As for opx, the Mg# is high, but displays little variation (0.939–0.946), which contrasts with the large variation in Cr# (0.181 to 0.294). The clinopyroxenes from Newfoundland are among the most depleted clinopyroxene from abyssal peridotites and peridotites from ocean–continent transition zones. They show substantial variation in Al_2O_3 (1.32 to 3.4), but relatively little variation for Na_2O (0.27–0.46) and TiO_2 (0.04 to 0.09). The clinopyroxene TiO_2 content is among the lowest ever found on the ocean floor.

Spinel is present in virtually all samples, either as porphyroclast or neoblast in a dynamically recrystallized matrix. Cores of large grains are usually unzoned, rim-

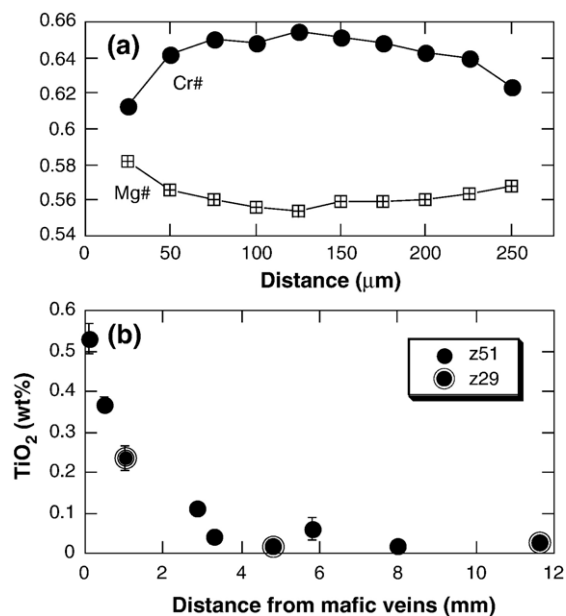


Fig. 4. (a) Compositional cross section of a small (~ 0.25 mm) spinel grain. Cr# and Mg# are homogeneous in the core, but are affected by re-equilibration at the outer ~ 50 μm (4R-1). (b) TiO_2 versus distance to small gabbroic dikes within the Newfoundland spinel harzburgites. Spinel $\text{TiO}_2 > 0.2$ wt.% is only observed within ~ 2 mm from gabbroic veins. In all other samples, including breccias, TiO_2 is below 0.15 wt.%, precluding equilibration within the plagioclase stability field. Error bars indicate 1σ variation of at least 3 measurements on individual grains.

towards a weak increase of Mg# and concomitant decrease of Cr# has been found (Fig. 4a). Within-sample variation is generally small, but can be significant in spinels from sedimentary breccias (e.g. sample z10, Table 2) and in the vicinity of small gabbroic dikes (Fig. 4b). Cr# varies from 0.35 to 0.66, Mg# correlate negatively with Cr# and varies from 0.54 to 0.71 for individual grains unaffected by gabbro veins. TiO_2 content is generally below 0.15 wt.%, with a few exceptions of spinel interacting with mafic veins (Fig. 4b). Compared to spinels from the Iberia margin, the Newfoundland spinels are TiO_2 poor, and also extend to higher Cr# (Fig. 5).

Fig. 4b illustrates spinel compositional variation as a function of the distance from gabbroic veins. Both samples show a consistent increase in TiO_2 with respect to the gabbroic veins. Spinel that are more than ~ 2 mm away from the gabbroic veins show background peridotite compositions. This is strong evidence that elevated TiO_2 contents in spinel from Newfoundland peridotite is related to the intrusion of mafic veins, and do not represent a primary feature.

Cr# of coexisting spinels and clinopyroxene are shown in Fig. 6, together with data from Iberia [16–

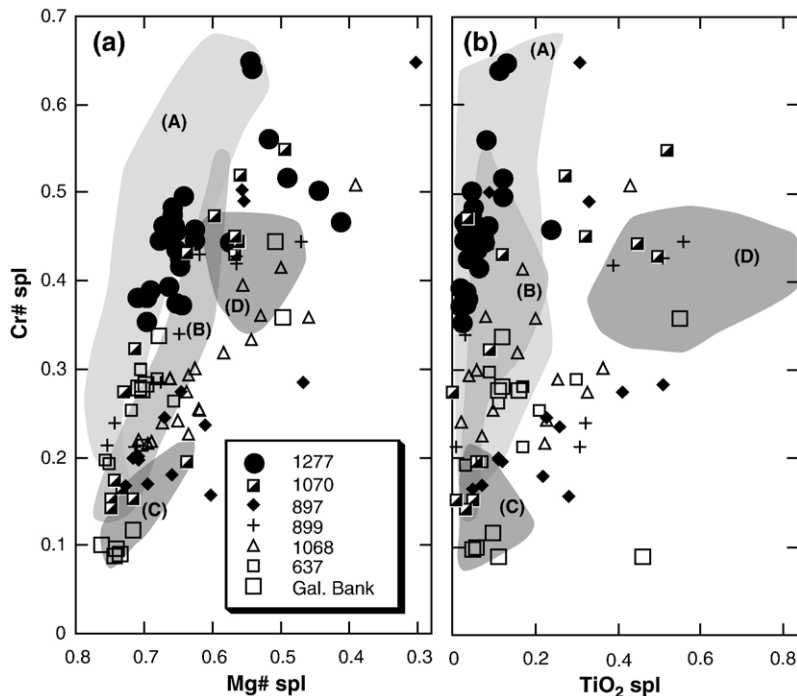


Fig. 5. (a) Cr# versus Mg# of spinels from the conjugated Iberia–Newfoundland rift. Cr# of Newfoundland spinels vary from 0.35 to 0.65. Note that the associated Mg# are generally low, thus precluding substantial low temperature Fe enrichment. Exceptions are related to mm-scale gabbroic veins, and dynamically recrystallized spinel in the matrix of 4R-1. (b) Cr# vs TiO₂ of spinels. Newfoundland spinels have TiO₂ contents below 0.15 wt.%. Spinel with TiO₂ > 0.2 are related to small gabbroic dikes. Note that high TiO₂ contents are found for all ODP sites from the Iberia margin, indicating equilibration in the plagioclase stability field. Shaded fields are from [37] (A), [25] (B), [8] and our unpublished data, (C) spinel peridotites, and (D) plagioclase peridotites. Data from Iberia from [16–18,23,24].

18,23,24], Alpine ophiolites [8, and our unpublished data], and abyssal peridotites [26]. Fig. 6 illustrates that Newfoundland spinels, on average, have higher Cr# in cpx and spinel than samples from Iberia. Spinel Cr# (up to 0.65) even exceeds those from the most depleted abyssal peridotites [26–28]. The positive correlation of Cr# in spinel and cpx is indicative of equilibration in the spinel peridotite field. The shift of spinel Cr# to the right of the spinel peridotite trend for many Iberia and Alpine peridotite samples reflects equilibration in the plagioclase peridotite field. The significance of the plagioclase peridotites in Iberia will be discussed below.

3.3. Temperature estimates

Equilibrium temperatures of Newfoundland harzburgites are subject to considerable uncertainty, because of the strong alteration of the samples. Temperatures estimated with defocused beam analyses of 20 μm on orthopyroxene porphyroclasts are variable and produced unsatisfactory results because of partial replacement of cpx lamellae by calcite (Fig. 3c). For this reason, only

focused beam analyses have been used and temperatures are calculated on the basis of mineral data summarized in Table 3. Although the application of the Ca-in-opx thermometer [29] might be problematic for some samples approaching cpx-out, it can be applied to the recrystallized, mylonitic assemblage in sample 4R-1, as both pyroxene coexist and are devoid of any exsolutions. Assuming a pressure of 1 GPa (above plagioclase stability), the temperatures estimated lie between 840 and 890 °C, with an average around 870 °C. Application of the Al–Cr in opx thermometer of Witt–Eickschen and Seck [30] to the samples listed in Table 3 gave values between 1030 and 1080 °C, with an average around 1050°. The low Al–Cr opx of sample 4R-1, however, is outside the limits where this thermometer can be applied [30]. Despite these shortcomings, the data indicate thermal equilibration of the spinel harzburgites at ~1050 °C, followed by dynamic recrystallization under decreasing temperatures of 850 to 900 °C. However, the temperatures are inconsistent with the estimated degree of melting (see below), and therefore we propose that the Newfoundland harzburgites have

been affected by post-melting thermal equilibration in the mantle lithosphere.

4. Discussion

We will first discuss the main differences between peridotites from the Newfoundland and Iberia margins by evaluating available mineral compositions. We then discuss the spatial variability of spinel peridotites across the Iberia–Newfoundland transect ~ 125 Ma ago and present hypotheses for their origin as residues of partial melting related to the opening of the Atlantic, or alternatively, as residues of a subduction-related magmatic arc related to the Caledonian or an older orogeny.

4.1. Degree of melting of Newfoundland spinel harzburgite

Spinel pyroxene relationships from Newfoundland and Iberia mantle rocks preserve features from both spinel and plagioclase peridotites. Because plagioclase is often altered in strongly serpentinized peridotites, it is difficult to determine the plagioclase peridotite–spinel peridotite ratio of a particular drill site from core description or thin section observations alone. We

therefore filtered the entire Newfoundland–Iberia dataset, somewhat arbitrarily, for spinels with $\text{TiO}_2 < 0.15$, and > 0.15 wt.%, and used this criteria to calculate the relative abundance of spinel peridotite from each site. We excluded spinel from pyroxenites and those occurring next to mafic dikes. The results of these calculations are illustrated in Fig. 7a. The uncertainties for each site are large, but the entire dataset shows that less than 40% of the analyzed Iberia samples have spinel $\text{TiO}_2 < 0.15$, while more than 98% of Newfoundland spinels have less than 0.15 wt.% TiO_2 . This is strong evidence that Newfoundland spinels are the residues of melting in the spinel peridotite field, without obvious late stage impregnation or reequilibration in the plagioclase stability field. This is also supported by the good correlation between the Cr# of spinel and clinopyroxene (Fig. 6), which extends to the high end of the global abyssal peridotite dataset [26–28], while such a correlation cannot be observed for plagioclase peridotite as found on the Iberian margin.

The remaining spinels with $\text{TiO}_2 < 0.15$ were used to calculate the degree of melting (f). There are two non-mutually exclusive approaches to determine f . One possibility is to couple peridotite REE melting models with spinel Cr#. Hellebrand et al. [31] have shown that the heavy REE of cpx from abyssal peridotites are highly correlated with spinel Cr#, and they presented a quantitative formulation of spinel Cr# vs. f . Such calculations are restricted to 4 phase spinel lherzolites and spinel Cr# between 0.1 and 0.6. An alternative possibility is to estimate the degree of melting from high-pressure experimental studies, which have shown that cpx-out occurs between 10 and 25% of partial melting for different mantle sources [13,32,33]. In all these studies, however, spinel Cr# exceeding 0.6 are rare in experimental studies of dry peridotite systems relevant for mantle melting.

Fig. 7b illustrates the calculated degree of melting for Newfoundland spinels with $\text{Cr}\# < 0.6$, together with data from Iberia. A modified version corrected for subsolidus effects has been used [27]. There is a clear difference between Newfoundland and Iberia spinels. First, the minimum f for Newfoundland samples is 14% but reaching up to 18%, while in Iberia much more fertile spinel lherzolites are preserved, with a few samples ($< 20\%$ of the entire dataset) displaying degrees of melting exceeding 10%. Second, Iberia spinel peridotites show a larger variability in the degree of partial melting, similar to many peridotite massifs that are exposed in ophiolites [8,34] and in ultra-slow spreading oceanic crust [27]. Such a large variation on vertical distances of less than 100 m (the maximum drilling depth of individual holes in

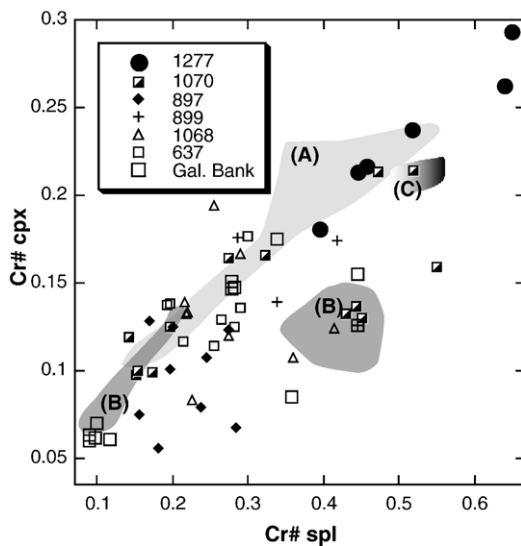
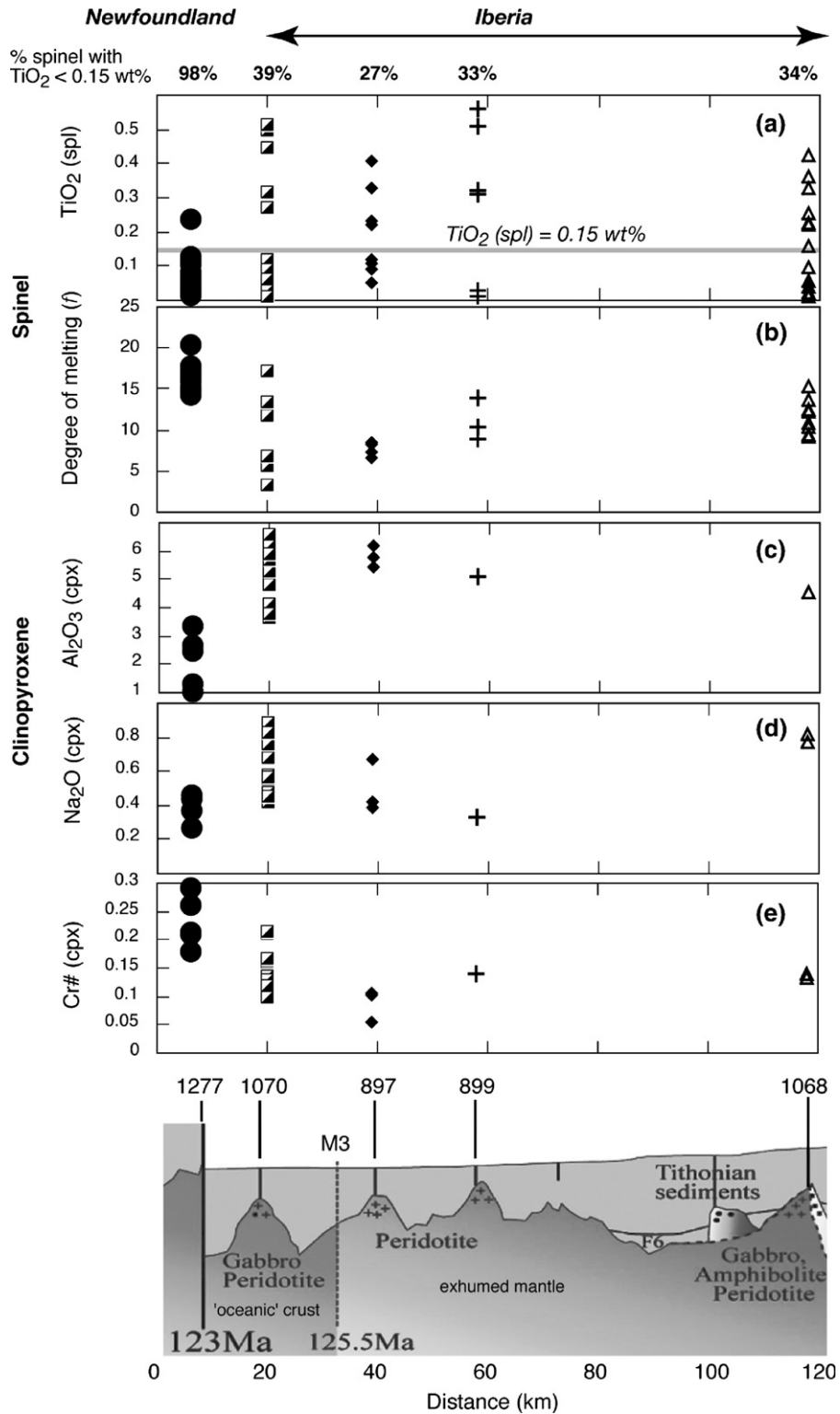


Fig. 6. Cr# of cpx versus associated spinel in peridotites from the Iberia–Newfoundland rift. Light shaded field (A) are spinel peridotites from the Lena trough [25]. Dark shaded field (B) are spinel and plagioclase peridotites from the Eastern Central Alps ([8] and our unpublished data) (C) is from [26]. All samples from Site 1277 are aligned along the Cr# covariation trend for spinel peridotites, while many samples from Iberia show substantial deviation towards higher Cr# in spinel. This offset results from partial equilibration with plagioclase. Data sources and symbols as in Fig. 5.

Iberia) is likely to be due to secondary enrichment processes, and cannot be explained by incomplete melt extraction of a partially molten peridotite.

Spinel Cr# exceeding 0.6 are extremely rare in abyssal peridotites (e.g. [35]) and have not been reported from the most depleted samples from the mid-Atlantic



ridge (ODP leg 209 [36]), the Gakkel ridge [27], and the East Pacific Rise (ODP leg 147, [26]. Although it is possible that dredged and drilled peridotite samples do not cover the entire variability found along slow spreading ridges in terms of spinel Cr# (Hellebrand, pers. comm.), we consider it unlikely that the depleted Newfoundland harzburgites formed in a ridge environment related to the opening of the southern North Atlantic, and there are two possible alternatives for the formation of such high Cr# spinels: (a) formation in a cratonic setting, or (b) formation in the sub-arc mantle. Below we evaluate these alternative interpretations further.

4.2. Possible origins of Newfoundland spinel harzburgites

To test whether the Newfoundland harzburgites could represent exhumed cratonic mantle, we compared East Greenland cratonic peridotite with our data (Fig. 5). Although there is some overlap of Newfoundland spinels with those reported by Bernstein et al. [37], a cratonic origin is unlikely, for two reasons: At a given spinel Cr# the Newfoundland spinel have, on average, lower Mg#. In addition, Mg# of pyroxenes and olivine from Newfoundland never reach the high Mg# reported from cratonic peridotites and are about 2% lower than these. An alternative explanation for high Cr# spinels is that they are residues formed by hydrous partial melting in the subarc mantle: Cr# exceeding 0.6 coupled with extremely Al-poor orthopyroxene is known from subduction-related peridotite massifs (e.g. Japan: Miyamori complex [38,39]; Papua New Guinea [40]; Newfoundland: parts of the Bay of island ophiolite, [35,41]. Hydrous partial melting of the mantle wedge at relatively shallow pressures would produce melt fractions substantially exceeding 20% without invoking extremely high temperatures, leaving a cpx-free harzburgite residue, consisting of Ca-poor pyroxene, olivine and Cr-rich spinel. As shown by several experimental studies, melt fractions exceeding cpx-out under dry conditions require substantially higher temperatures than reasonable estimates of adiabatic upper mantle temperatures beneath ridges (for a review, see [12]). Such high temperatures

are uncommon among abyssal peridotites (e.g. [26,42]). We conclude that, at least for samples with spinel Cr# >0.6, the Newfoundland peridotites acquired their residual signature in an environment other than a mid-ocean ridge, possibly in an arc environment.

4.3. Spatial variability of peridotite composition across the Iberia–Newfoundland conjugate margin

In Fig. 7, the conjugate magma poor passive margins of Iberia and Newfoundland are rearranged to illustrate the spatial relationships of spinel and pyroxene data from the Newfoundland magma-poor passive margin, together with previously published data from Iberia [16–18,23,24]. These data show systematic chemical variations across the margin as a function of distance (~120 km), at the time of magnetic anomaly M1 (~121 Ma). Despite the limited number of peridotite samples from Iberia with coexisting cpx and low TiO₂ spinel, there is a tendency of more fertile mantle minerals being preserved in Iberia (Fig. 7c–e). Cpx from Iberia has Al₂O₃ >4%, while cpx from Newfoundland has <4 wt.% Al₂O₃. Similar results can be obtained from opx (not shown here). The largest chemical variability is shown by Site 1070, which seems transitional between depleted spinel harzburgites from Newfoundland and more fertile samples close to the thinned continental crust (e.g. Site 1068). It was suggested that (syn-rift) melt percolation caused variability in mineral chemistry and led to coarsening of the peridotite textures at Site 1070 [23], while this is clearly not the case on Site 1277, where peridotites are rather homogeneous and preserve a porphyroclastic to mylonitic high temperature foliation. Local melt infiltration and equilibration at shallow pressures (in the plagioclase peridotite facies), coupled with recrystallization and coarsening would explain why mantle peridotites on Iberia are heterogeneous, however, this is debated. Most studies on the plagioclase peridotites from Iberia consider an exclusively metamorphic origin of plagioclase by cold, subsolidus deformation related to extension [16,18,43], while others emphasize, that plagioclase might have a ‘dualistic’ origin [17,44]. The hypothesis of local melt

Fig. 7. Spatial variability of spinel and clinopyroxene compositions across the Iberia–Newfoundland passive margin, reconstructed to anomaly M1 (~123 My, after [19]). The samples represent a cross section of approximately 120 km between Site 1277 and Site 1068. (a) Spinel TiO₂ for spinel and plagioclase peridotites (excluding pyroxenites). Numbers indicate spinel analyses with TiO₂ <0.15, in % of the total spinel analyses from the different peridotite sites (sources of data as in Fig. 5). (b) Calculated degree of melting after [27]: Only samples with coexisting cpx and low Ti spinel (TiO₂ <0.15 wt.%) are considered. Note that spinels from Iberia indicate that there are remnants of fertile peridotite (e.g. degree of melting <8% for some samples), while Newfoundland samples all indicate high degrees of melting. (c, d, e) Compositional variability of cpx coexisting with spinel (TiO₂ <0.15 wt.%); Newfoundland cpx show the lowest Al₂O₃ and Na₂O, and the highest Cr#, indicating the most residual compositions of the Iberia–Newfoundland system.

infiltration on Iberia would also explain the contrast in bulk rock compositions of peridotites from Iberia and Newfoundland [23,45,46].

4.4. Inherited high degrees of melting: Caledonian or older? Possible origins of subarc mantle exposed on the Newfoundland margin

The high degree of melting ($14 < f < \sim 25\%$) of Newfoundland peridotite is in apparent conflict with the minor volumes of basaltic mafic rocks drilled from Site 1277. Whole rock analyses of basaltic flows on top of the peridotite indicate a transitional MORB composition [47] somewhat less enriched than basalts from site 897 and 899 [48,49]. In all drill sites of the conjugate Iberia–Newfoundland margin, volumes of erupted magmas are low (< 1 km), and the trace element chemistry of recovered basalts requires relatively low degrees of mantle melting. It thus appears that the peridotite basement of the Newfoundland margin records high degrees of melt extraction, while the mafic rocks provide little evidence of being produced by high degrees of mantle melting. Whatever the ultimate origin of the Newfoundland peridotite, the high degrees of mantle melting is inconsistent with the simplest assumption that the ‘oceanic crust’ at Site 1277 is genetically related to the peridotite basement immediately beneath. Instead, we propose that the drilled Newfoundland mantle peridotites record a pre-rift (subduction-related) history that might be related to the Caledonian, or an older orogenic event. Evidence for Caledonian (subduction-related) magmatism is present at the East Coast of Nova Scotia and Newfoundland (e.g. [50,51]). We tentatively propose that the drilled peridotites were exhumed from beneath the Newfoundland continental crust, during the rifting evolution of the Iberia–Newfoundland passive margin, along large scale shear zones. The relatively high degrees of melting formed a mantle lithosphere that might be compositionally buoyant, similar to cratonic lithosphere [52,53]. Although highly speculative, the overall different basement topography of the Newfoundland margin compared to the Iberia margin might be accentuated by ‘inherited buoyancy’, a hypothesis, which is generally consistent with the compositional differences between the Iberia and Newfoundland peridotite.

5. Conclusions

The Newfoundland peridotites are highly depleted spinel harzburgites, with a minimum degree of melting of $\sim 14\%$ up to melting degrees approaching cpx-out at

$\sim 25\%$, that acquired their geochemical signature prior to the extensional evolution of the Iberia–Newfoundland rift, most probably in a subduction-related magmatic arc. As a consequence, the mafic rocks that are covering the top of the peridotite basement at Site 1277 are genetically unrelated to the exposed mantle rocks.

There is neither textural nor geochemical evidence of refertilization/equilibration in the plagioclase stability field on the Newfoundland margin. Pyroxene equilibration temperatures vary between ~ 1050 °C for porphyroclasts, and ~ 850 °C for the mylonitic equilibration. Such a cold deformation history is consistent with exhumation of mantle rocks on the seafloor via passive extension.

The near-absence of volcanic products on Site 1277 and elsewhere on the Newfoundland–Iberia margin indicates that decompression melting of the underlying asthenosphere was subdued, until at least the formation of presumed oceanic crust (e.g. at M3). This can either be explained by a low mantle potential temperature, by a refractory composition of the peridotite or by a combination of both. Exhumation of depleted (arc) peridotites might be a general mechanism to suppress the formation of syn-rift melts.

Acknowledgements

This research used samples provided by the Ocean Drilling Program (ODP), which is sponsored by funding agencies of the participating countries under management of Joint Oceanographic Institutions (JOI), Inc. This research was supported by Swiss National Science Foundation grants (PP002-102809). We thank Brian Tucholke and Jean-Claude Sibuet for support, Réjean Hébert for making his Iberia dataset available to us, Donna Shillington and Harm Van Avendonk for conversations on seismic aspects of the Newfoundland margin, the participants of the postcruise meeting in Briançon 2005 for inspiring and controversial discussions, and Eric Hellebrand for a constructive review.

References

- [1] G. Boillot, M. Recq, E.L. Winterer, A.W. Meyer, J. Applegate, et al., Tectonic denudation of the upper mantle along passive margins: a model based on drilling results (ODP leg 103, western Galicia margin, Spain), *Tectonophysics* 132 (1987) 335–342.
- [2] G. Boillot, S. Grimaud, A. Mauffret, D. Mougenot, J. Komprobst, J. Mergoil-Daniel, G. Torrent, Ocean–continent boundary off the Iberian Margin: a serpentinite diapir west of the Galicia Bank, *Earth Planet. Sci. Lett.* 48 (1980) 23–34.
- [3] B.E. Tucholke, J. Lin, M.C. Kleinrock, Megamullions and mullion structure defining oceanic metamorphic core complexes

- on the Mid-Atlantic ridge, *J. Geophys. Res.* 103 (1998) 9857–9866.
- [4] B.E. Tucholke, K. Fujioka, T. Ishihara, G. Hirth, M. Kinoshita, Submersible study of an oceanic megamullion in the central North Atlantic, *J. Geophys. Res.* 106 (2001) 16145–16161.
- [5] E. Bonatti, D. Brunelli, P. Fabretti, M. Ligi, R.A. Portaro, M. Seyler, Steady-state creation of crust-free lithosphere at cold spots in mid-ocean ridges, *Geology* 29 (2001) 979–982.
- [6] P.J. Michael, C.H. Langmuir, H.J.B. Dick, J.E. Snow, S.L. Goldstein, D.W. Graham, K. Lehnert, G. Kurras, W. Jokat, R. Muhe, H.N. Edmonds, Magmatic and amagmatic seafloor generation at the ultraslow-spreading Gakkell ridge, Arctic Ocean, *Nature* 423 (2003) 956–961.
- [7] H.J.B. Dick, J. Lin, H. Schouten, A new class of mid-ocean ridges, *Nature* 426 (2003) 405–412.
- [8] O. Müntener, T. Petke, L. Desmurs, M. Meier, U. Schaltegger, Refertilization of mantle peridotite in embryonic ocean basins: trace element and Nd-isotopic evidence and implications for crust–mantle relationships, *Earth Planet. Sci. Lett.* 221 (2004) 293–308.
- [9] M. Cannat, F. Chatin, H. Whitechurch, G. Ceuleneer, Gabbroic rocks trapped in the upper mantle at the mid-atlantic ridge, in: J.A. Karson, M. Cannat, D.J. Miller, D. Elthon (Eds.), *Proc. ODP, Sci. Res.*, vol. 153, 1997, pp. 243–264.
- [10] P.B. Kelemen, Shipboard Scientific party, Igneous crystallization beginning at 20 km beneath the Mid-Atlantic ridge, 14–16N, EOS, *Trans. AGU*, 2004.
- [11] M.M. Hirschmann, Mantle solidus: experimental constraints and the effects of peridotite composition, *Geochem. Geophys. Geosyst.* 1 (2000) (2000GC000070).
- [12] P. Ulmer, Partial melting of the mantle wedge — the role of H₂O in the genesis of mantle-derived ‘arc-related’ magmas, *Phys. Earth Planet. Inter.* (2001) 215–232.
- [13] L.E. Wasylenki, M.B. Baker, A.J.R. Kent, E.M. Stolper, Near-solidus melting of the shallow upper mantle: partial melting experiments on depleted peridotite, *J. Petrol.* 44 (2003) 1163–1191.
- [14] J.W. Bown, R.S. White, Variation with spreading rate of oceanic crustal thickness and geochemistry, *Earth Planet. Sci. Lett.* 121 (1994) 435–439.
- [15] T.A. Minshull, S.M. Dean, R.S. White, R.B. Whitmarsh, Anomalous melt production after continental breakup in the southern Iberia Abyssal Plain, in: R.C.L. Wilson, R.B. Whitmarsh, B. Taylor, N. Froitzheim (Eds.), *Non-volcanic Rifting of Continental Margins: a Comparison of Evidence from Land and Sea*, vol. 187, *Geol. Soc. of London, Spec. Publ.*, 2001, pp. 537–550.
- [16] J. Kornprobst, A. Tabit, Plagioclase bearing ultramafic tectonites from the Galicia margin (Leg 103 Site 637): comparison of their origin and evolution with low-pressure ultramafic bodies in Western Europe, *Proc. Ocean Drill. Program Sci. Results* 103 (1988) 252–268.
- [17] G. Cornen, M.O. Beslier, J. Girardeau, Petrologic characteristics of the ultramafic rocks from the ocean–continent transition in the Iberia abyssal plain, in: R.B. Whitmarsh, D.S. Sawyer, A. Klaus, D.G. Masson (Eds.), *Proceedings of the Ocean Drilling Program, Scientific Results*, vol. 149, 1996, pp. 377–395.
- [18] G. Chazot, S. Charpentier, J. Kornprobst, R. Vannucci, B. Luais, Lithospheric mantle evolution during continental break-up: the West Iberia non-volcanic passive margin, *J. Petrol.* 46 (2005) 2569–2592.
- [19] B. Tucholke, J.-C. Sibuet, A. Klaus, et al., *Proceedings of the Ocean Drilling Program, Initial reports*, vol. 210, 2004 http://www-odp.amu.edu/publications/210_IR/210ir.htm.
- [20] D.J. Shillington, W.S. Holbrook, H.J.A. Van Avendonk, B.E. Tucholke, J.R. Hopper, K.E. Loudon, H.C. Larsen, G.T. Nunes, O.L.S. Party, Evidence for asymmetric non-volcanic rifting and slow incipient seafloor spreading from seismic reflection data on the Newfoundland margin, *J. Geophys. Res.* 111 (in press) B09402, doi:10.1029/2005JB003981.
- [21] H.J.A. Van Avendonk, W.S. Holbrook, G.T. Nunes, D.J. Shillington, B. Tucholke, K.E. Loudon, H.C. Larsen, J.R. Hopper, Seismic velocity structure of the rifted margin of the eastern Grand Banks of Newfoundland, Canada, *J. Geophys. Res.* (in press).
- [22] O. Jagoutz, O. Müntener, G. Manatschal, G. Péron-Pinvidic, D. Rubatto, I.M. Villa, The rift-to-drift transition in the Atlantic: A stuttering start of the MORB engine? (in preparation).
- [23] R. Hébert, K. Gueddari, M.R. Laflèche, M.O. Beslier, V. Gardien, Petrology and geochemistry of exhumed peridotites and gabbros from non-volcanic margins: ODP leg 173 West Iberia ocean–continent transition zone, in: R.C.L. Wilson, R.B. Whitmarsh, B. Taylor, N. Froitzheim (Eds.), *Non-volcanic Rifting of Continental Margins: a Comparison of Evidence from Land and Sea*, vol. 187, *Geol. Soc. London, Spec. Publ.*, 2001, pp. 161–189.
- [24] N. Abe, Petrochemistry of serpentinized peridotite from the Iberia Abyssal plain (ODP Leg 173): its character intermediate between sub-oceanic and subcontinental upper mantle, in: R.C.L. Wilson, R.B. Whitmarsh, B. Taylor, N. Froitzheim (Eds.), *Non-volcanic Rifting of Continental Margins: A Comparison of Evidence from Land and Sea*, vol. 187, *Geol. Soc. London, Spec. Publ.*, 2001, pp. 143–159.
- [25] E. Hellebrand, J.E. Snow, Deep melting and sodic metasomatism underneath the highly oblique-spreading Lena Trough (Arctic Ocean), *Earth Planet. Sci. Lett.* 216 (2003) 283–299.
- [26] H.J.B. Dick, J.H. Natland, Late stage melt evolution and transport in the shallow mantle beneath the East Pacific Rise, in: K. Gillis, C. Mevel, J. Allan, et al., (Eds.), *Scientific Results*, vol. 147, *Ocean Drilling Program, Texas A&M University, College Station, TX*, 1996, pp. 103–134.
- [27] E. Hellebrand, J.E. Snow, S. Mostefaoui, P. Hoppe, Trace element distribution between orthopyroxene and clinopyroxene in peridotites from the Gakkell ridge: a SIMS and NanoSIMS study, *Contrib. Mineral. Petrol.* 150 (2005) 486–504.
- [28] E. Hellebrand, J.E. Snow, P. Hoppe, A.W. Hofmann, Garnet-field melting and late-stage refertilisation in ‘residual’ abyssal peridotites from the Central Indian ridge, *J. Petrol.* 43 (2002) 2305–2338.
- [29] G.P. Brey, T. Köhler, Geothermobarometry in four-phase lherzolites II. New thermobarometers, and practical assessment of existing thermobarometers, *J. Petrol.* 31 (1990) 1353–1378.
- [30] G. Witt-Eickschen, H.A. Seck, Solubility of Ca and Al in orthopyroxene from spinel peridotite: an improved version of an empirical geothermometer, *Contrib. Mineral. Petrol.* 106 (1991) 431–439.
- [31] E. Hellebrand, J.E. Snow, H.J.B. Dick, A.W. Hofmann, Coupled major and trace elements as indicators of the extent of melting in mid-ocean-ridge peridotites, *Nature* 410 (2001) 677–681.
- [32] K. Hirose, I. Kushiro, Partial melting of dry peridotites at high pressures: determination of compositions of melts segregated from peridotite using aggregates of diamond, *Earth Planet. Sci. Lett.* 114 (1993) 477–489.
- [33] T.J. Falloon, D.H. Green, Anhydrous partial melting of peridotite from 8 to 35 kb and the petrogenesis of MORB, *J. Petrol.* (1988) 379–414.
- [34] J.L. Bodinier, Geochemistry and petrogenesis of the Lanzo peridotite body, Western Alps, *Tectonophysics* 149 (1988) 67–88.

- [35] H.J.B. Dick, T. Bullen, Chromian spinel as a petrogenetic indicator in abyssal and alpine-type peridotites and spatially associated lavas, *Contrib. Mineral. Petrol.* 86 (1984) 54–76.
- [36] G. Suhr, H. Paulick, Upper mantle geochemistry at peridotites of site 1274 (ODP leg 209): relation to melt-rock reaction and processes at the base of the lithosphere, *EOS Transactions, American Geophysical Union*, 2004 V22A-06.
- [37] S. Bernstein, P.B. Kelemen, K. Brooks, Depleted spinel harzburgite xenoliths in Tertiary dykes from East Greenland: restites from high degree melting, *Earth Planet. Sci. Lett.* 154 (1998) 221–235.
- [38] K. Ozawa, Ultramafic tectonite of the Miyamori ophiolitic complex in the Kitakami Mountains, Northeast Japan: hydrous upper mantle in an island arc, *Contrib. Mineral. Petrol.* 99 (1988) 159–175.
- [39] K. Ozawa, Melting and melt segregation in the mantle wedge above a subduction zone: evidence from the chromite-bearing peridotites of the Miyamori Ophiolite Complex, northeastern Japan, *J. Petrol.* 35 (1994) 647–678.
- [40] R.N. England, H.L. Davies, Mineralogy of ultramafic cumulates and tectonites from eastern Papua, *Earth Planet. Sci. Lett.* 17 (1973) 416–425.
- [41] J.H. Bédard, Cumulate recycling and crustal evolution in the Bay of Islands ophiolite, *J. Geol.* 99 (1991) 225–249.
- [42] P.C. Hess, Phase equilibria constraints on the origin of ocean floor basalts, in: J. Phipps Morgan, D.K. Blackman, J.M. Sinton (Eds.), *Mantle Flow and Melt Generation at Mid-Ocean Ridges*, Geophysical Monograph, vol. 71, American Geophysical Union, Washington, D.C., 1993, pp. 67–102.
- [43] M.O. Beslier, G. Cornen, J. Girardeau, Tectono-metamorphic evolution of peridotites from the ocean–continent transition of the Iberia Abyssal plain margin, in: R.B. Withmarsh, D.S. Sawyer, A. Klaus, D.G. Masson (Eds.), *Proceedings of the Ocean Drilling Program*, Scientific Results, vol. 149, 1996, pp. 397–412.
- [44] G. Cornen, J. Girardeau, C. Monnier, Basalts, underplated gabbros and pyroxenites record the rifting process of the West Iberian margin, *Mineral. Petrol.* 67 (3–4) (1999) 111–142.
- [45] A. Engström, Fluid–rock interaction history and geochemical structure of ODP leg 210, Site 1277, ODP Leg 210, 2nd Post-ruise Meeting, Briançon, France, 2005, p. 9.
- [46] K. Seifert, D. Brunotte, Geochemistry of serpentinized mantle peridotite from site 897 in the Iberia Abyssal plain, in: R.B. Withmarsh, D.S. Sawyer, A. Klaus, D.G. Masson (Eds.), *Scientific Results*, vol. 149, Ocean Drilling Program, Texas A&M University, College Station, TX, 1996, pp. 413–424.
- [47] A.H.F. Robertson, Earliest formed slow spreading rifted oceanic crust: sedimentary, igneous and structural evidence from the Newfoundland rifted margin, in: *Scientific Results*, B.E. Tucholke, J.-C. Sibuet, eds. 210, pp. in press, Ocean Drilling Program, Texas A&M University, College Station, TX.
- [48] G. Cornen, M.O. Beslier, J. Girardeau, Petrology of the mafic rocks cored in the Iberia Abyssal plain, in: R.B. Withmarsh, D.S. Sawyer, A. Klaus, D.G. Masson (Eds.), *Proceedings of the Ocean Drilling Program*, Scientific Results, vol. 149, 1996, pp. 449–469.
- [49] K. Seifert, C.W. Chang, D. Brunotte, Evidence from Ocean Drilling Program Leg 149 mafic igneous rocks for oceanic crust in the Iberia Abyssal Plain ocean–continent transition zone, *J. Geophys. Res.* 102 (1997) 7915–7928.
- [50] D. Elthon, Geochemical evidence for formation of the Bay of Islands ophiolite above a subduction zone, *Nature* 354 (1991) 140–142.
- [51] G. Pe-Piper, L.F. Jansa, Pre-Mesozoic basement rocks offshore Nova Scotia, Canada: new constraints on the accretion history of the Meguma terrane, *Geol. Soc. Amer. Bull.* 111 (12) (1999) 1773–1791.
- [52] T.H. Jordan, The continental tectosphere, *Rev. Geophys.* 13 (1975) 1–12.
- [53] T.H. Jordan, Composition and development of the continental tectosphere, *Nature* 274 (1978) 544–548.
- [54] S.P. Shrivastava, J.-C. Sibuet, S. Cande, W.R. Roest, I.R. Reid, Magnetic evidence for slow seafloor spreading during the formation of the Newfoundland and Iberian margins, *Earth Planet. Sci. Lett.* 182 (2000) 61–76.